CHEMISTRY
A EUROPEAN JOURNAL

DOI: 10.1002/chem.200701042

Investigation of Hydrogen Physisorption Active Sites on the Surface of Porous Carbonaceous Materials

Deyang Qu*[a]

Abstract: Hydrogen physisorption in different carbonaceous materials was investigated in liquid nitrogen (77 K). The total hydrogen adsorption was found to have a linear relationship with the surface area of pores <30 Å. The surface area and porosity of the carbon materials were determined by dinitrogen adsorption at 77 K and density function theory (DFT). The active sites for hydrogen adsorption were investigated and found to be related to the edge orientation of defective graphene micro-sheet domains.

Keywords: active sites · hydrogen adsorption · monolayers · physisorption · porous carbon

Introduction

Energy and water, in particular their shortage, clean generation, and biocomplex environmental impact, are two pressing global challenges. Hydrogen, which can be produced from renewable sources and which burns pollution-free, is gaining increasing attention as a solution to these challenges. Hydrogen storage is a crucial and technically challenging step to providing a ready supply of hydrogen fuel for end use, and it is a problem that remains unresolved after decades of exploration. The current approaches to hydrogen storage include:[1–6]

- Gaseous and liquid hydrogen storage via compression or liquefaction under cryogenic conditions.
- Chemical storage in irreversible hydrogen carriers.
- Reversible metal and chemical hydrides.
- Gas-on-solid adsorption.

The operating requirements for effective hydrogen storage include appropriate thermodynamics, fast kinetics, high storage capacity, effective heat transfer, high gravimetric and volumetric densities, a long cycle lifetime for hydrogen uptake/release, high mechanical strength and durability, safety under normal use, acceptable risk under abnormal conditions and, most importantly, hydrogen adsorption/desorption under near-ambient conditions.[1] Unfortunately, none of the above-mentioned approaches can satisfy all the requirements, even though each method possesses desirable characteristics in certain areas.

Alongside other materials, carbon, especially carbon nanotubes, has been extensively studied for hydrogen storage and some very exciting results have been reported. Dillon et al. reported 5 wt% of H_2 storage at 273 K in single-walled carbon nanotubes (SWNTs).[7] Liu et al. reported a H_2 storage capacity of 4.2% in SWNTs.[8] Ye et al. found that 8.25 wt% of hydrogen can be stored in high-purity SWNTs at 80 K under about 7 MPa.[9] 13 wt% of hydrogen storage was reported by Chen et al. in multiwalled carbon nanotubes (MWNTs).[10] Alkali metal-doped nanotubes have been reported to store up to 20 wt% of hydrogen.[11] The highest reported H_2 storage capacity in carbon materials so far is 67% in graphite nanofibers by Chambers et al.[12] However, other researchers have not been able to reproduce these results and reported hydrogen storage capacities in carbon nanotubes are scattered over several orders of magnitude.[13,14] For example, the work done by Chen on hydrogen uptake by alkali-doped carbon nanotubes[11] has not been reproduced by other researchers and it was subsequently proved that the majority of the weight gain was due to moisture that the alkali oxide had picked up from the atmosphere.[15,16] Recently, H_2 physisorption in different carbon nanostructures was investigated by using classical Monte-Carlo simulation techniques. Less than 1 wt% uptakes have been calculated for SWNTs, MWNTs, and graphite nanofibers at 293 K and 10 MPa.[17] Assuming that

[a] D. Qu
Department of Chemistry
University of Massachusetts
100 Morrissey Boulevard
Boston, MA, 02125 (USA)
Fax: (+1) 617-287-6185
E-mail: Deyang.qu@umb.edu

hydrogen condenses as a monolayer on the surface of nanotubes and also that bulk condensation occurs in the cavity of the tubes, 5 wt % uptakes were calculated.[18] However, hydrogen condensation may only occur under cryogenic conditions. In addition to the uncertain capacity, H_2 adsorption and desorption kinetics may be a limiting factor as well, due to the H_2 diffusion rate inside the carbon nanotubes. Indeed, the practical use of nanotubular materials is dubious at best, owing to the cost, limited scale of production, and uncertain purity.

Gas-on-solid adsorption is an inherently safe and potentially energy-dense hydrogen-storage method that could be extremely energy efficient. Hydrogen storage in high surface area activated carbon materials is very pertinent and has been extensively studied.[19–22] Hydrogen can be physically adsorbed onto carbon materials by a van der Waals interaction with a binding energy of around 0.1 eV.[20] Given the intrinsic difficulty of tuning the carbon surface–H_2 van der Waals interaction to compete with thermal energies, the vast majority of the sites for adsorption cannot stabilize hydrogen and because of this, the development of carbon-based adsorbents for hydrogen storage is extremely challenging. It is necessary to enhance the carbon–H_2 interaction without sacrificing the desorption kinetics. However, the mechanism of H_2 physisorption on the carbon surface, especially surface–H_2 interactions and the surface energy, is not well understood. This paper focuses not only on the impact of carbon porosity, but also on the influence of the crystal structure of the carbon material, which has not been reported. The "active site" for hydrogen physisorption will also be discussed.

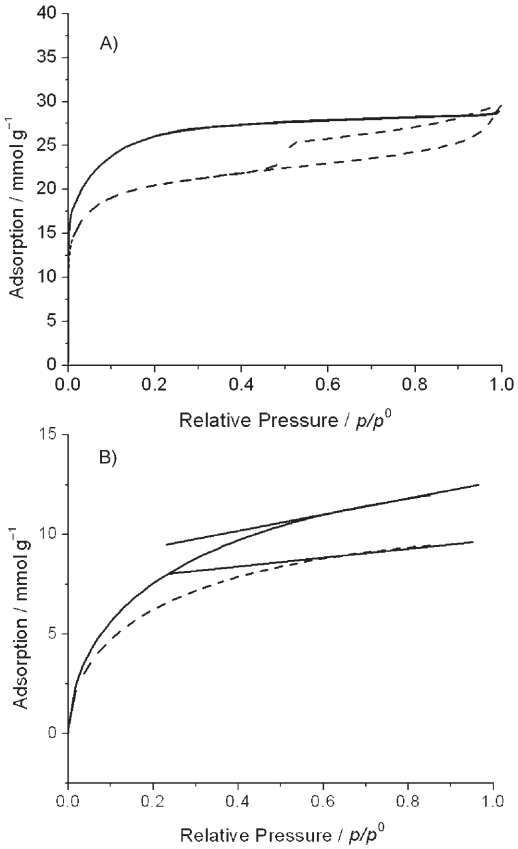

Figure 1. A) The nitrogen adsorption isotherms at 77 K for two activated carbon materials; M20: —— and U-2b: – – –. B) The hydrogen adsorption isotherms at 77 K for the same carbon materials; M20: —— and U-2b: – – –.

Results and Discussion

Nitrogen adsorption isotherms: Figure 1 shows the adsorption isotherms of the activated carbon materials M20 and U-2b, which represent two types of the large surface area carbon materials used in the study. Figure 1A shows the comparison of N_2 adsorption isotherms for M20 and U-2b at 77 K. The isotherm for M20 represents a typical Type I isotherm,[23] which is characterized by a nearly-horizontal plateau. Type I isotherms are given by microporous solids that have a relatively small external surface area, for which the limiting uptake of N_2 is governed by the accessible micropore volume rather than by the internal surface area. The isotherm for U-2b shows an ideal Type IV isotherm.[23] The characteristic feature is the hysteresis loop, which is associated with capillary condensation taking place in the mesopores. Type IV isotherms are given by adsorbents with mesopores. Figure 1B shows the comparison of H_2 adsorption isotherms for the same carbon materials at 77 K. The H_2 adsorption isotherms for both carbon materials are close to the characteristics of a Type II isotherm,[23] which represents unrestricted monolayer adsorption. Type II is usually characteristic of a nonporous or possibly macroporous material. It is reasonable to assume that the adsorption of hydrogen onto the surface of pores of various sizes forms a monolayer at 77 K. Unlike nitrogen adsorption, which forms multiple layers through condensation and volume filling,[24] hydrogen condensation and volume filling may not occur in micro- and mesopores. This can be explained by examining the critical temperatures for nitrogen and hydrogen, which are 126.2 and 32.98 K, respectively. Thus, nitrogen may condense in meso- and micropores at 77 K, but hydrogen would only condense below a temperature of 33 K. The amount of hydrogen adsorbed at 0.9 relative pressure (120 Pa) was reported as the hydrogen adsorption capacity.

Porosity and surface area of an activated carbon: Various carbon materials have unique pore distributions, which result from the precursors and processes involved. Pores are formed within the particles of a fine powder, the primary particles,[24] or in the aggregated secondary particles that are formed when primary particles stick together. The total surface area of a fine powder is the sum of the pore wall area of all the pore sizes. Although there are a number of techniques available for surface-area measurements, for example, mercury intrusion and small-angle X-ray diffraction, the most commonly used tool for the purpose is still a gas ad-

sorption isotherm, for example, nitrogen adsorption. For most high-surface-area carbon materials, the macropore contribution to the total surface area is negligible compared with that of meso- and micropores. Nitrogen adsorption onto the surface of micropores is fundamentally different to that of mesopores. The nitrogen adsorption of micropores results from volume filling,[24] whereas nitrogen molecules condense into mesopores through a classical capillary effect. The major difference between the volume filling of micropores and capillary condensation in mesopores is the strong cooperative behavior of the filling gas in the micropores, which is absent in the mesopores due to the relative weakness of the molecular–molecular and molecular–wall interaction. Instead of the phenomenological approaches, such as the Brunauer–Emmett–Teller (BET) equation, it is more acceptable to use a molecular-based statistical thermodynamic theory that relates the adsorption isotherm to the microscopic properties of the system, that is, the fluid–fluid and fluid–solid interaction energy parameters, the pore size, pore geometry, and the temperature. In this report, a model based on density function theory (DFT) is used to extract the pore-size distribution from the nitrogen adsorption isotherm. DFT is based on the idea that the free energy of an inhomogeneous fluid can be expressed as a function of $\rho(r)$. Once the functional is known, all the relevant thermodynamic functions can be calculated and the microscopic structure of the inhomogeneous fluid can also be determined.[25,26] With the aid of fast computers, the whole adsorption isotherm can be fitted and the pore-size distribution can be calculated. Figure 2 shows the comparison of the pore-size distribution profiles for M20 and U-11b, calculated from the DFT model. These two carbon materials were chosen to demonstrate the significant difference in micropore distribution. The incremental surface area has contributions from pores with a range of sizes between 5 and 50 Å (5 Å is the smallest size that can be measured by the nitrogen adsorption method). The incremental surface area contribution from pores of a certain size range can be obtained from Figure 2.

Physical adsorption of hydrogen: It has been reported that hydrogen adsorption is proportional to either the total surface area or the micropore volume of the activated carbon, and also that at 77 K, the activated carbon surface can be treated as a uniform flat surface and H_2 physisorption forms a monolayer.[1,6,27–29] However, after the careful analysis of hydrogen adsorption onto various carbon materials at 77 K (see Table 1), the adsorption capacity was actually found to be proportional to the surface area of pores <30 Å. Figures 3A–C show the correlation between the H_2 adsorption capacity and the surface area for pores <30, <100 (total surface area), and <10 Å (micropores), respectively. It appears that the H_2 adsorption capacity has the best linear relationship with the surface area of pores <30 Å. Neither the total surface area nor the micropore surface area show linear correlation with the H_2 adsorption capacity. Figure 4 shows the relationship between the total H_2 adsorption capacity and the average pore size of different activated carbon materials. The total adsorption decreases with the increase of pore size until it reaches about 30 Å. The total percentage of H_2 adsorbed changes little for carbon materials with an average pore size larger than 30 Å. The result in Figure 4 is in good agreement with that of Figure 3. One may assume that the majority of H_2 becomes adsorbed on the wall of pores <30 Å in size.

Table 1. Adsorption data for the activated carbon materials used in this study.

Carbon	Surface area <10 nm	Surface area <30 nm	Total surface area [nm]	Adsorption at $p/p^0=0.5$	Adsorption at $p/p^0=0.9$
APD	520.2	874.0	941.1	1.5	1.3
m30	581.7	1363.0	1486.9	2.1	1.9
m20	876.7	1435.1	1450.0	2.3	2.1
M1470	570.4	702.6	783.0	1.4	1.3
Nor-A	652.4	1166.6	1211.0	1.9	1.7
PWA	497.3	691.4	718.0	1.4	1.2
SC2220	867.5	1470.8	1478.0	2.3	1.99
SC2225	716.9	1485.7	1491.6	1.9	1.7
WPH	518.8	839.6	904.0	1.5	1.3
U-1B	546.0	609.0	631.0	1.2	1.2
U-2B	658.6	1122.7	1179.4	1.9	1.7
U-6B	628.7	926.0	957.5	1.5	1.4
U-11B	572.5	1290.0	1349.0	1.8	1.6
U-L1-I3	431.2	1150.0	1437.1	1.7	1.5
U-T2	689.8	962.0	996.1	1.5	1.4
U-T7	487.7	1206.0	1355.0	1.8	1.6
U-T7b	499.3	1100.0	1130.0	1.7	1.5
U-T13	536.7	720.3	755.7	1.3	1.2

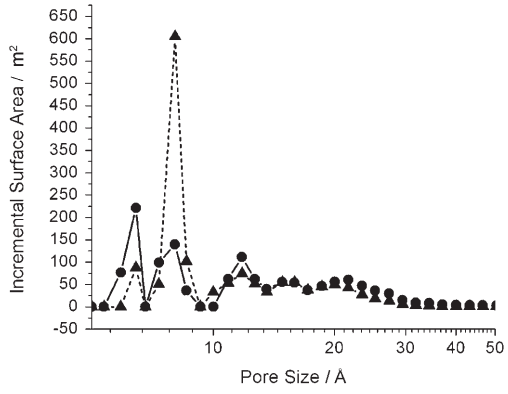

Figure 2. A comparison of pore size distribution obtained from two activated carbon materials using a DFT method; M20: ——●—— and U-11b: – – –▲– – –. The pores were assumed to be slit-pores.

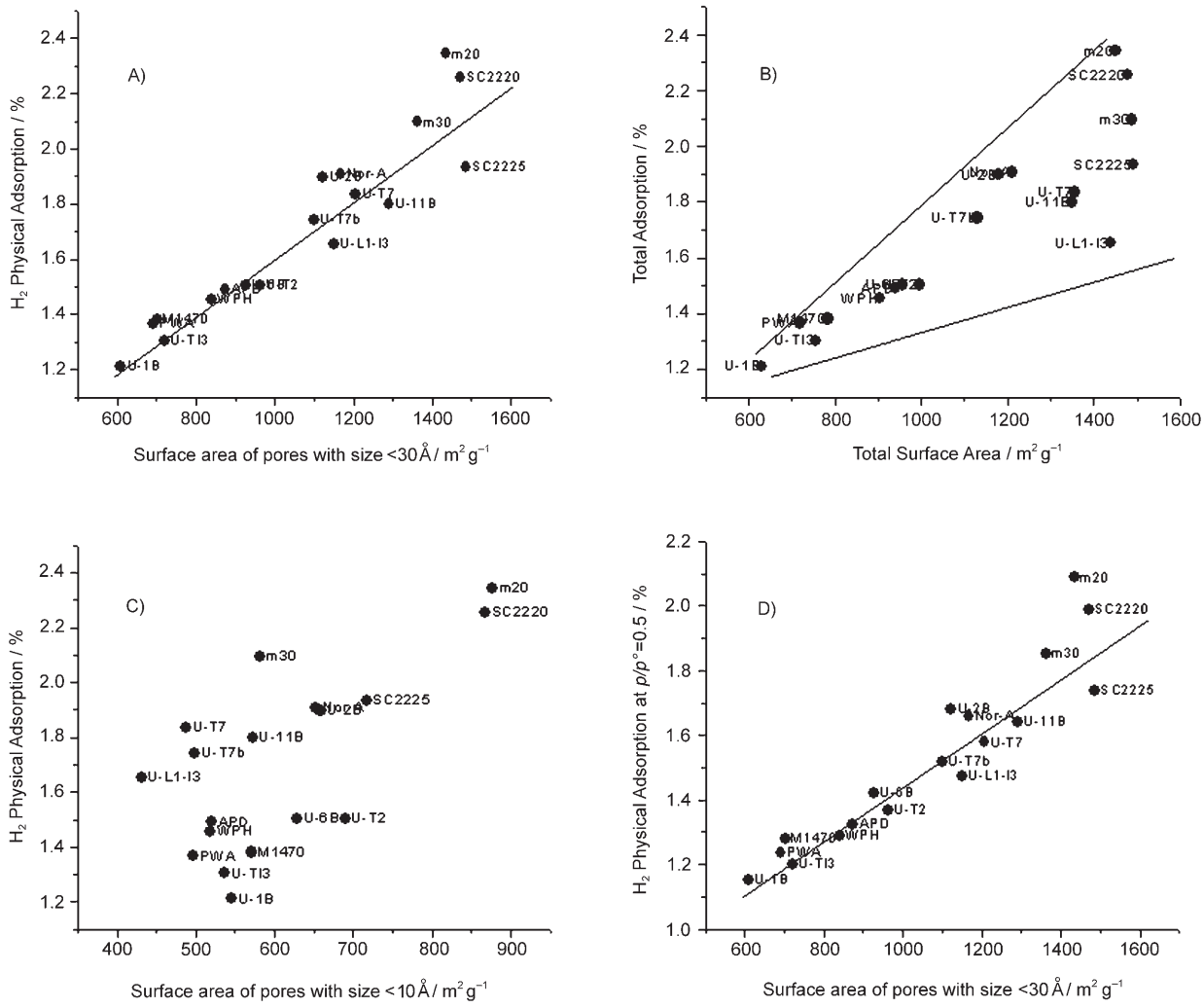

Figure 3. A–C) Graphs of hydrogen adsorption versus surface area at 77 K. Surface area = pore size < 30 Å, total surface area, and pore size < 10 Å, respectively. D) Hydrogen adsorption ($p/p^0 = 0.5$, 77 K) versus surface area of pores < 30 Å.

It is worth emphasizing that the maximum applied hydrogen pressure in this study was about 1.20 kPa. Hydrogen molecules formed a sub-monolayer on the surface of carbon material, because the available adsorption sites were not yet fully saturated. Higher pressure would be needed to form a monolayer. After the formation of a monolayer, H_2 adsorption capacity should have a better linear relationship with the total surface area.[19] However, as shown in Figure 1B, the amount of H_2 adsorbed on the surface of both carbon materials increases linearly with the applied pressure, starting from a relative pressure of roughly 0.5. Figure 3D shows the correlation between H_2 adsorbed at 0.5 relative pressure and the surface area of pores < 3 nm. A linear relationship similar to that in Figure 1A is demonstrated. It is reasonable to conclude that the surface area contributions from pores < 30 Å play a dominant role in H_2 adsorption at 77 K. Even though high pressure may be needed for monolayer adsorption, at 77 K the majority of H_2 becomes adsorbed on the surface area of pores < 30 Å at a pressure lower than 60 kPa.

To understand these phenomena, the surface energy and the wall–adsorbate interaction need to be investigated in detail. The hypothesis is that the enhancement results from the curvature effect. This effect could occur in pores that are narrow enough for the whole of the adsorbate to be in range of the forces originating from the solid surface. At this distance, the influence of the surface is still present and the potential fields from neighboring walls would overlap, so the interaction energy of the solid with a gas molecule would be correspondingly enhanced. The hydrogen molecules in such pores could, therefore, have modified properties that result from the surface force effects on the chemical potential of the adsorbate. However, such curvature effects only occur in microporous solids that have capillaries with a width not exceeding a few molecular diameters. As such adsorption fields fall off fairly rapidly with distance from the surface, the building-up of the monolayer should not be affected by the presence of a neighboring surface situated at a significantly large distance.

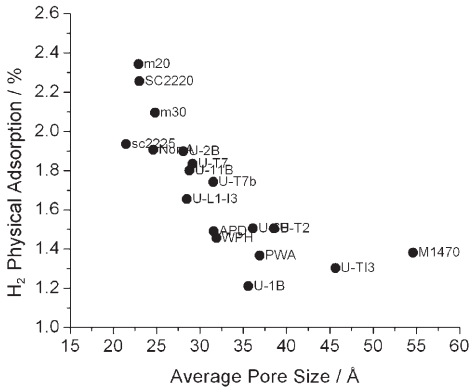

Figure 4. Hydrogen adsorption (77 K) versus average pore size for a selection of activated carbon materials.

The main objective of the investigation was to understand the active sites for molecular hydrogen adsorption. Figure 5 shows the relationship between specific H_2 adsorption

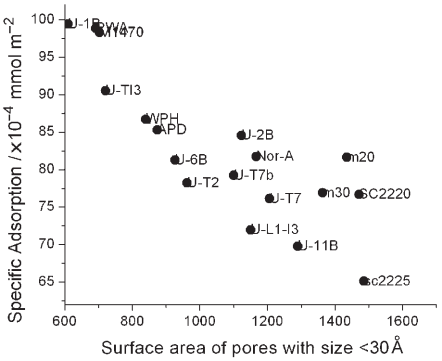

Figure 5. Specific hydrogen adsorption ($mmol\,m^{-2}$) versus surface area of pores <30 Å.

($mmol\,m^{-2}$) and the surface area contribution from pores <30 Å at 77 K. Although the relationship is not good, the specific adsorption varies, which means the density of active sites on the surface of different carbon materials varies.

The structure of activated carbon materials: Activated carbon materials with large activated surface areas consist of sheets of small hexagonal carbon rings, called "graphene sheets". Unlike the graphene sheets in graphitized carbon, the graphene sheet in activated carbon is highly defective and may not even be planar. The structure of carbon is composed of roughly parallel associations of hydrocarbon moieties and quite defective nonplanar, but roughly parallel, associations of carbon atoms. Carbon materials made from different precursors and different preparation methods lead to different sizes, orientation, and stacking arrangements of these defective micrographene sheets. In general, however, an activated carbon has an amorphous structure and lacks long-range three-dimensional order. An activated carbon can be considered as molecular space, this space being contained within a three-dimensional network of carbon atoms that are arranged in layers composed of range structures joined together somewhat imperfectly. This network is continuous in three dimensions, with some layers being stacked, roughly parallel to each other, in groups of up to two or three, usually not more.[30]

To graphically explain the short-range arrangement within a high-surface-area amorphous carbon material, Dahn et al. proposed a "falling cards" model to explain the complex structure of activated carbon.[31] This model treats activated carbon as the combination of a lot of small domains that consist of a few graphene sheets in parallel. These sheets are formed by breaking the links between adjacent graphene sheets and allowing some sheets to rotate into parallel orientations. It should be mentioned that activated carbon materials are usually non-graphitizable or "hard" carbon, so the possibility of considerable movement or alignment of the graphene sheets within a solid matrix at the activation temperature (about 1000 °C) is unlikely. However, from the powder XRD patterns of the activated carbon materials studied in this paper (see Figure 6), the (100) peak at 42° and the (110) peak at 79° can be clearly observed, indicating that these materials consist of small domains of ordered graphene sheets. To estimate the number of carbon sheets arranged as single layers, Dahn et al.[31] proposed an empirical parameter (R) which is defined as the ratio of the height of the (002) Bragg peak to the background, as illustrated in Figure 6. It has been demonstrated by the researchers that R decreases as the single-layer content of the carbon increases. When $R=1$, all graphene layers are randomly distributed as single layers, so the R value is proportional to the amount of edge orientation on the carbon surface. Larger R values indicate a higher percentage of edge orientation, since higher R values result from more graphene sheets stacking in parallel, which results in increased edge exposure on the carbon surface. According to Dahn's model, all activated carbon materials studied in this paper should contain randomly oriented single- and multilayer domains.

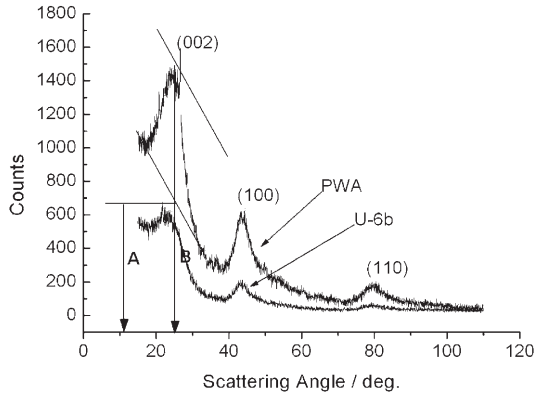

Figure 6. Comparison of XRD profiles for activated carbon materials PWA and U-6b, for which the relative amount of edge orientation $R=B/A$.

The active site for hydrogen adsorption: The active site describes that volume element of which one adsorbate molecule may reside. It relates to the adsorption potential at the location of the site, which is the effective control. The size and orientation of the defective micrographene sheets may play an important role in the adsorption process by altering the London dispersion forces between the surface and hydrogen molecules. The surface porosity may be related to the presentation of the domains of the defective micrographene layers, since some of the sheets may present their basal planes and others may present the edge layers. The surface energy is related to crystal orientation (edge/basal exposure), surface defects, functional groups, and surface curvature of pores of various sizes. This lack of homogeneity may create more favorable sites for H_2 adsorption. Even though the interaction between the hydrogen molecule and the carbon surface is a van der Waals force, the surface-energy distribution of carbon materials may not be homogeneous, thus the strength of H_2–surface interactions varies. Thus, the hypothesis is that the active sites for hydrogen adsorption onto the surface of carbon materials are mainly the edge orientations of microdomains.

Figure 7 shows the relationship between *R* value and the specific physical adsorption ($mmol\,m^{-2}$). It clearly demonstrates that specific hydrogen adsorption increases with the *R* value, in other words, higher edge exposure on the carbon surface results in increased physical H_2 adsorption per square meter, which is consistent with the hypothesis. It is worth emphasizing that physisorption results from van der Waals interactions between the carbon surface and the hydrogen molecule. Unlike chemisorption, in which hydrogen molecules are stabilized through bond formation, the hydrogen molecules adsorbed through van der Waals interactions are in a dynamic equilibrium. At an active site of adsorption, the residence time of the adsorbed molecule is longer than that of the surrounding sites. Any local enhancement of the interaction force can result in longer residence times. On the edge plane, for which all the surface atoms have unsaturated bonds, the surface energy would be significantly greater than that of the basal layer for which no free valencies remain. Two things could happen on the edge plane: higher London dispersion forces between the surface and the hydrogen molecules or more surface functional groups could be observed. Both will result in longer H_2 residence time by enhancing the carbon–H_2 interaction. Besides the edge orientation, any local defects in the basal plane of the defective microsheet can also enhance the local interaction force for the same reason. It should be pointed out that H_2 could also be physically adsorbed onto a flat basal plane, but the van der Waals forces would be weaker, which makes the basal plane sites less favorable for hydrogen physical adsorption.

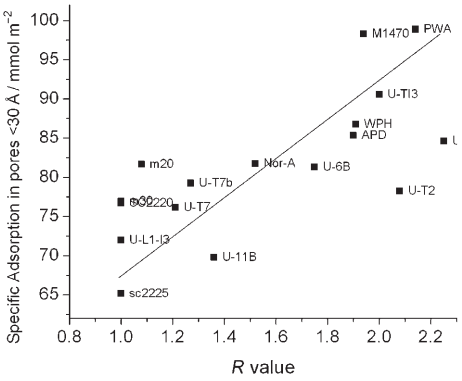

Figure 7. Specific hydrogen adsorption versus *R*.

Conclusion

Various high surface area carbon materials have been investigated for hydrogen adsorption at 77 K. Instead of depending on the total surface area reported in literature, the total percentage of hydrogen physically adsorbed depends almost linearly on the surface area ($m^2\,g^{-1}$) of pores <30 Å in size. The specific adsorption ($mmol\,m^{-2}$) depends on the carbon nanostructure. Therefore, the physical hydrogen adsorption process is based on local interactions between the hydrogen molecules and the active sites. The edge orientation of defective microsheet domains contributes a significant number of active sites for hydrogen residence. The physisorption of hydrogen molecules at 77 K is determined by short-range order, curvature, functional groups, ordered arrays of defective graphene microsheets, and possibly defects on the basal layer of the graphene sheets.

Experimental Section

Various carbon materials were obtained from different suppliers or modified in-house, to cover a wide range of porosity and crystal structures. For example, M20 was obtained from Spectracorp (USA) and U-2b and U-11b were from Emtech (Canada). All activated carbon materials were reflux-washed with acetone in a Soxhlet extractor for 48 h to remove most of the weakly-bonded surface functional groups that remained from the precursors and the manufacturing process.

Gas adsorption isotherms were measured by using a Micromeritics ASAP 2020 porosimeter. Nitrogen was used as the adsorbate gas for surface and porosity analysis. Density function theory (DFT) software from Micromeritics was used to calculate pore size distributions from the N_2 adsorption isotherms. During the hydrogen adsorption measurement, the sample was first placed under vacuum to a pressure of 0.00013 Pa with a high-vacuum pump, then hydrogen was doped to a series of preset relative pressures until the pressure reached 120 kPa ($p/p^0=0.9$, p^0 was arbitrarily set as 133.3 kPa). The amount of hydrogen adsorbed was recorded after the system had reached thermal equilibrium. All measurements were done in liquid nitrogen. All samples were subjected to eight-hour programmed vacuum degassing at 280 °C before the measurements and a liquid nitrogen cold trap was used to make sure that trace amounts of water vapor in the adsorbate were removed. The void volume of a sample tube was determined by helium adsorption.

The X-ray powder diffraction patterns of each sample were collected with a Siemens D5000 powder diffractometer equipped with a Cu target X-ray tube and monochromator.

Acknowledgement

The financial support of this work by UMass (Boston) through the Joseph P Healey Grant is gratefully acknowledged.

[1] L. Schlapbach, A Zuttel, *Nature* **2001**, *414*, 353–358.
[2] M. S. Dresselhaus, K. A. Williams, P. C. Eklund, *MRS Bull.* **1999**, *24*, 45–50 (issue 11).
[3] M. Bououdina, D. Grant, W. Walker, *Int. J. Hydrogen Energy* **2006**, *31*, 177–182.
[4] A. C. Dillon, M. J. Heben, *Appl. Phys. A* **2001**, *72*, 133–142.
[5] A. Zuttel, P. Wenger, P. Sudan, P. Mauron, S.-i. Orimo, *Mater. Sci. Eng. B* **2004**, *108*, 9–18.
[6] M. Conte, P. P. Prosini, S. Passerini, *Mater. Sci. Eng. B* **2004**, *108*, 2–8.
[7] A. C. Dillon, K. M. Jones, T. A. Bekkedahl, C. H. Kiang, D. S. Bethune, M. J. Heben, *Nature* **1997**, *386*, 377–379.
[8] C. Liu, Y. Y. Fan, M. Liu, H. T. Cong, H. M. Cheng, M. S. Dresselhaus, *Science* **1999**, *286*, 1127–1129.
[9] Y. Ye, C. C. Ahn, C. Witham, B. Fultz, J. Liu, A. G. Rinzler, D. Colbert, K. A. Smith, R. E. Smalley, *Appl. Phy. Lett.* **1999**, *74*, 2307–2309.
[10] Y. Chen, D. T. Shaw, X. D. Bai, E. G. Wang, L. Lund, W. M. Lu, D. D. L. Chung, *Appl. Phys. Lett.* **2001**, *78*, 2128–2130.
[11] P. Chen, X. Wu, J. Lin, K. L. Tan *Science* **1999**, *285*, 91–93.
[12] A. Chambers, C. Park, R. Terry, K. Baker, N. M. Rodriguez, *J. Phys. Chem. B* **1998**, *102*, 4253–4256.
[13] X. Li, H. Zhu, L. Ci, C. Xu, Z. Mao, B. Wei, J. Liang, D. Wu, *Carbon* **2001**, *39*, 2077–2079.
[14] M. Hirscher, M. Becher, M. Haluska, U. Dettlaf-Weglikowska, A. Quintel, G. S. Duesberg, Y.-M. Choi, P. Downes, M. Hulman, S. Roth, I. Stepanex, P. Bernier, *Appl. Phys. A* **2001**, *72*, 129–132.
[15] F. E. Pinkerton, B. G. Wicke, C. H. Olk, G. G. Tibbetts, G. P. Meisner, M. S. Meyer, J. F. Herbst, *J. Phys. Chem. B* **2000**, *104*, 9460–9467.
[16] R. T. Yang, *Carbon* **2000**, *38*, 623–626.
[17] P. Guay, B. L. Stansfield, A. Rochefort, *Carbon* **2004**, *42*, 2187–2193.
[18] A. Zuettel, A. Sudan, P. Mauron, P. Wenger, *Appl. Phys. A* **2004**, *78*, 941–946.
[19] B. Panella, M. Hirscher, S. Roth, *Carbon* **2005**, *43*, 2209–2214.
[20] S. Orimo, A. Zuttel, L. Schlapbach, G. Majer, T. Fukunaga, H. Fujii, *J. Alloys Compd.* **2003**, *356–357*, 716–719.
[21] H. Takagi, H. Hatori, T. Yamada, *Carbon* **2005**, *43*, 3037–3039.
[22] E. Terres, B. Panella, T. Hayashi, Y. A. Kim, M Eudo, J. M. Dominguez, M. Hirscher, H. Terrones, M. Terrones, *Chem. Phys. Lett.* **2005**, *403*, 363–366.
[23] K. S. W. Sing, D. H. Everett, R. A. W. Haul, L. Moscou, R. A. Pierotti, J. Rouguerol, T. Siemieniewska, *Pure Appl. Chem.* **1985**, *57*, 603–619.
[24] S. J. Gregg, K. S. W. Sing, *Adsorption, Surface Area and Porosity*, Academic Press, London, **1982**.
[25] P. A. Webb, C. Orr, *Analytical methods in fine particle technology*, Micromeritics Instrument Corporation, GA. **1997**; pp. 53–91.
[26] J. S. Oliver, *J. Porous Mater.* **1995**, *2*, 9–17.
[27] R. Strobel, L. Jorissen, T. Schliermann, V. Trapp, W. Schutz, K. Bohmhammel, G. Wolf, J. Garche, *J. Power Sources* **1999**, *84*, 221–224.
[28] N. Texier-Mandoki, J. Dentzer, T. Piquero, S. Saadallah, P. David, C. Vix-Guterl, *Carbon* **2004**, *42*, 2735–2737.
[29] J. M. Blackman, J. W. Patrick, A. Arenillas, W. Shi, C. E. Snape, *Carbon* **2006**, *44*, 1376–1385.
[30] H. Marsh, F. Rodrigues-Reinoso, *Activated Carbon*, Elsevier, New York, **2006**, p. 71.
[31] Y. Liu, J. X. Xue, T. Zheng, J. R. Dahn, *Carbon* **1996**, *34*, 193–200.

Received: July 6, 2007
Published online: November 12, 2007

